

Correspondence of Theoretical Models of Longitudinal Rod Vibrations to Experimental Data

A. L. Popov^{a,*} and S. A. Sadovsky^{b,**}

^a *Ishlinsky Institute for Problems in Mechanics, Russian Academy of Sciences, Moscow, 119526 Russia*

^b *Moscow State University of Civil Engineering, Moscow, 129337 Russia*

**e-mail: popov@ipmnet.ru*

***e-mail: bigostart@rambler.ru*

Received July 6, 2020; revised September 8, 2020; accepted December 17, 2020

Abstract—There are several theoretical models for describing longitudinal vibrations of a rod. The simplest and most common model is based on the wave equation. Less common is the model taking into account lateral displacement (Rayleigh correction). The Bishop model is considered to be superior, considering both transverse displacement and shear deformation. It would seem that the more improved the theoretical model, the better its agreement should be with experimental data. However, that turns out not to be quite the case when compared to an actual experimental spectrum of longitudinal rod vibrations over a large base of natural frequencies. Moreover, the most complex Bishop model turns out to be relatively weak. Comparisons were made for a smooth long cylindrical rod. Also discussed are the questions of specifying the velocity of longitudinal waves and Poisson's ratio of the rod material using experimentally obtained frequencies.

Keywords: rod, longitudinal vibrations, wave equation, Rayleigh correction, Bishop correction, experimental data

DOI: 10.1134/S1063454121020114

INTRODUCTION

The study of longitudinal vibrations of a rod has an extensive theoretical foundation. It is enough to mention classic monographs [1–3]. The most common and simple model for describing them is the wave equation. It assumes that the transverse dimensions of the rod are small compared to its length. This allows us to discard the effect of transverse deformations accompanying expansion-compression deformations during longitudinal vibrations when determining the longitudinal displacements of the rod.

The improved equation, which considers the transverse deformation during longitudinal rod vibrations, is derived in [2]. The resulting correction for the vibration frequencies coincides with the Rayleigh correction derived from energy considerations [1].

A generalization of the Rayleigh model is the model proposed by Bishop [4] for an unbounded rod, in which, along with transverse deformations, shear deformations are also taken into account. Unlike the other two, this model is described by a fourth-order differential equation in the longitudinal coordinate. The boundary conditions for the longitudinal vibration equation with the Bishop correction are given in [5]. Experimental studies of longitudinal vibrations of rods originate from Kundt's experiments performed using a tube invented by him [6]. Since then and up to the present time, two methods of vibration excitation are used: by a short-term shock action, causing freely decaying vibrations of the rod (method of free vibrations), or by continuous action with a smoothly varying frequency (resonance method) [7]. With the advent of modern spectrum analyzers, the first method that allows one to immediately and with high accuracy determine a large number of natural frequencies becomes preferable. Using this method, we consider the correspondence of theoretical models of longitudinal rod vibrations to experimental data. Three models are considered in order of increasing complexity.

BASIC THEORETICAL MODEL BASED ON THE WAVE EQUATION

To describe free longitudinal vibrations of a rod with a constant cross section, the wave equation is usually used in form [2]

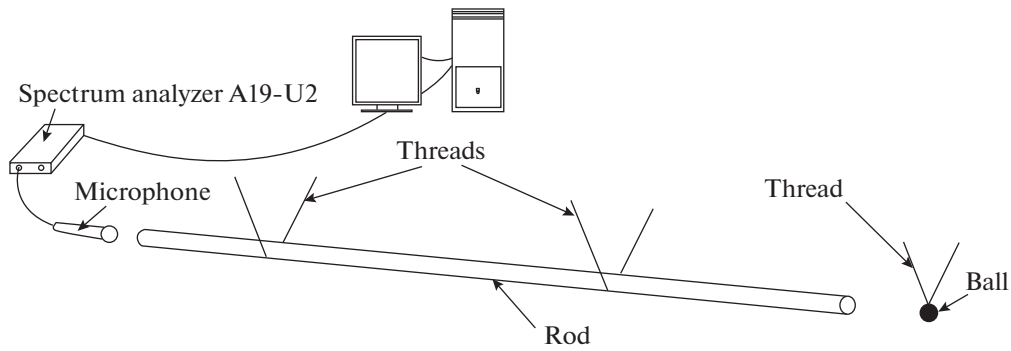


Fig. 1 Diagram of the setup.

$$\frac{\partial^2 u}{\partial t^2} = c^2 \frac{\partial^2 u}{\partial x^2}, \quad c = \sqrt{\frac{E}{\rho}}, \quad (1)$$

in which $u = u(x, t)$ is the longitudinal displacement of a point of the rod with coordinate x directed along its axis at time t , E is the modulus of elasticity, and ρ is the rod density. In the case of harmonic vibrations of the rod with circular frequency, the solution to this equation can be represented in form

$$u(x, t) = (C_1 \cos \lambda x + C_2 \sin \lambda x) \exp(i\omega t), \quad \lambda = \omega/c, \quad i = \sqrt{-1}, \quad (2)$$

where C_1 and C_2 are constants determined from the boundary conditions at the ends of the rod.

At rod ends $x = 0$ and l , let us set either fixing condition $u = 0$ or free end condition $\partial u / \partial x = 0$. By substituting solution (2) into these conditions, formulas are derived for the natural frequencies of longitudinal rod vibrations. In this case, only the rod vibration frequencies with a combination of free–free (F–F) and free–fixed (F–C) ends differ in the type of boundary conditions:

$$f_n = \frac{c}{2l} \left\{ \begin{array}{cc} n, & F - F \\ n - 1/2 & F - C \end{array} \right\}, \quad f_n = \frac{\omega_n}{2\pi}, \quad n = 1, 2, \dots \quad (3)$$

The vibration frequencies of a rod with fixed and free ends coincide [1].

The conditions of the free ends are most easily implemented in experiments, for example, when the rod is horizontally suspended on two threads (Fig. 1). Using rod vibrations under such conditions is also convenient because the resulting frequency spectrum, as Rayleigh pointed out [1], consists of alternating vibrational frequencies of a rod of half-length l with fixed–free and free–free ends. Note that the step between frequencies is the same, equal to the first frequency of a rod of length l with a fixed–free end.

EXPERIMENTAL MEASUREMENT OF THE LONGITUDINAL ROD VIBRATION SPECTRUM

The vibrations of a rod suspended on two threads were excited by the impact of a hardened steel ball on one of the ends of the rod (Fig. 1). Oscillations were recorded using a laboratory microphone installed near the other end. The signal from the microphone was transmitted to the A19-U2 spectrum analyzer and then to the computer, where it was processed using the ZETLab software [8].

The sample was a straight cylindrical rod made of aluminum alloy with a length of $L = 2006$ mm and a diameter of $d = 24.8$ mm. Figure 2a shows a fragment of a microphone recording of a multifrequency signal of rod sound emission with a duration of 0.2 s after impact at time $t = 0$, and Fig. 2b, shows the graphic rendition of the spectrum of this signal in Hz (the amplitudes along the ordinate axes are plotted in units of the electrical signal (mV) transmitted from the microphone). From Fig. 2b it can be seen that the distance between the pronounced discrete components in the obtained spectrum of vibration frequencies of the rod is almost constant, which corresponds to a uniform distribution of theoretical frequencies of longitudinal vibrations (3). However, upon detailed consideration, the experimental frequency distribution does not completely obey this simple law, and with an increase in the frequency number, there is an increase in the differences between the calculated and experimental values of frequencies.

It is also clear that with this method of excitation and registration of vibrations, the natural frequencies of other types of vibrations, for example, transverse, almost do not appear, despite the fact that the vibra-

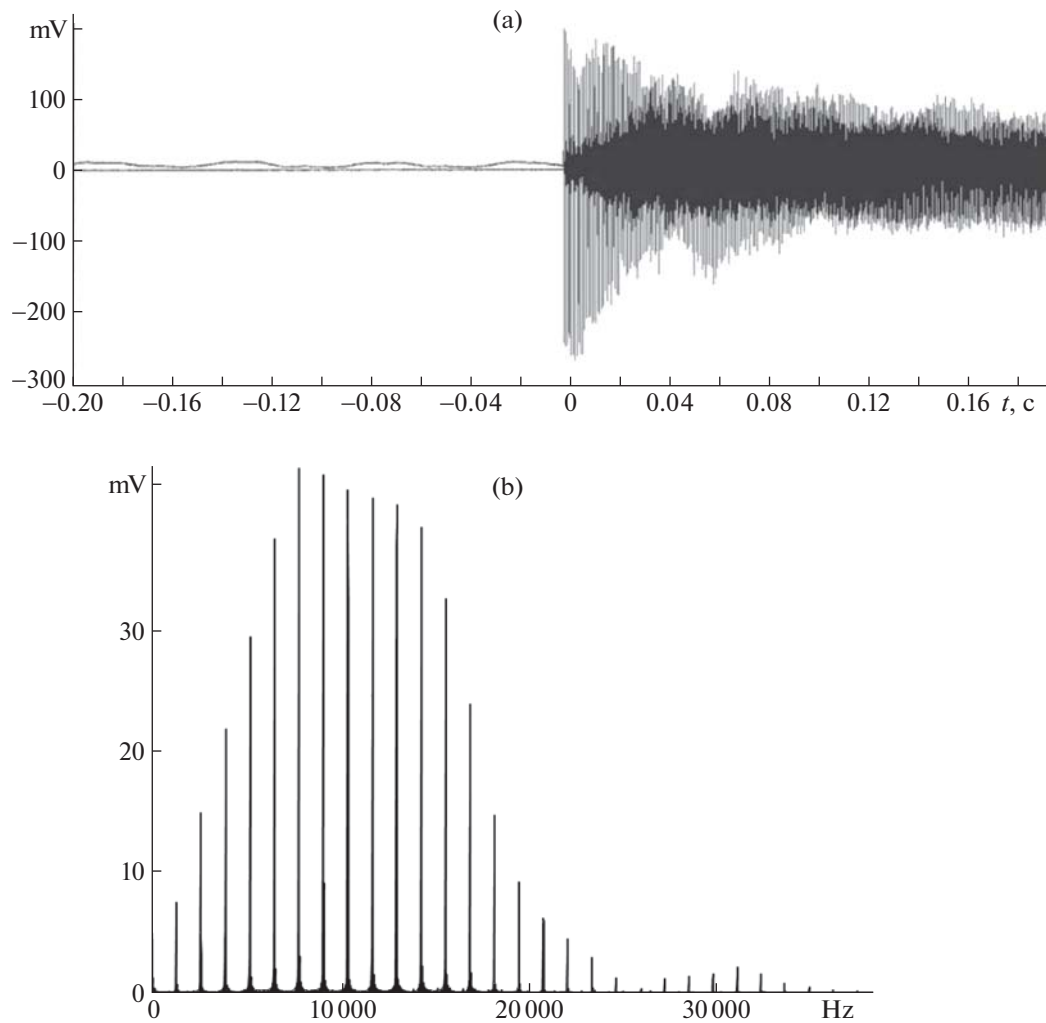


Fig. 2. Microphone recording with a duration of 0.2 s of a multifrequency signal of sound emission of a rod after impact on its end (a), spectrum of this signal in Hz (b).

tion spectrum is recorded starting from the lowest frequencies (from 20 Hz). However, it is possible that for other combinations of length and end boundary conditions, parametric resonance, found theoretically in [9], can occur; in that case significant transverse vibrations might arise.

COMPARISON OF EXPERIMENTAL AND THEORETICAL VIBRATION FREQUENCIES

For a numerical comparison of the experimental and theoretical frequencies of rod vibrations in formula (3), the velocity of compression-expansion waves c must be known, which is determined from (1) using the modulus of elasticity and the density of the rod material. The reference values for these parameters vary somewhat [10]: $E = (69\text{--}72.5)$ GPa, $\rho = (2650\text{--}2850)$ kg/m³. This leads to variation of values for the velocity of longitudinal waves in interval (4980–5230) m/s.

To determine the speed of sound in a rod more precisely, it was calculated using the experimentally obtained natural vibration frequency and rod length, an approach that was first implemented in Kundt's tube [6]. Using the first experimental frequency of longitudinal rod vibrations $f_{1, \text{exp}} = 1297.812$ Hz, we get from (3) velocity $c = 5206.822$ m/s. The rest of the calculated frequency values, as follows from (3), are determined by multiplying the first frequency by their numbers.

Table 1 shows the ratios of 30 experimentally recorded frequencies of longitudinal vibrations of the rod to the first frequency.

Table 1.

Frequency number (n)	1	2	3	4	5	6	7	8	9	10
$f_{n, \text{exp}}/f_1$	1.000	2.000	3.000	4.000	5.000	5.999	6.997	7.996	8.994	9.990
Frequency number (n)	11	12	13	14	15	16	17	18	19	20
$f_{n, \text{exp}}/f_1$	10.998	11.982	12.978	13.972	14.966	15.958	16.949	17.940	18.929	19.918
Frequency number (n)	21	22	23	24	25	26	27	28	29	30
$f_{n, \text{exp}}/f_1$	20.905	21.889	22.873	23.855	24.835	25.814	26.791	27.766	28.739	29.710

The table shows a gradual increase in the differences between the calculated and experimental frequencies, depending on the frequency number. By the 30th frequency (38 557.99 Hz), they already reach about 400 Hz, despite the fact that we consider a deliberately long rod with a length-to-diameter ratio of more than 80 and the wave equation can be applied without doubt for calculating its frequencies of longitudinal vibrations.

The increase in the differences between the calculated and experimental frequencies, depending on the frequency number, can be explained by the fact that the influence of the transverse deformation of the rod is not considered in the wave equation. This is fixed by introducing the Rayleigh correction, which can be obtained from the equation of the improved theory of longitudinal rod vibrations.

RAYLEIGH CORRECTION

The improved theory of longitudinal rod vibrations additionally considers the inertia of transverse displacements arising according to the Poisson effect. The equation of the improved theory of longitudinal rod vibrations has form [2]

$$\frac{\partial^2 u}{\partial t^2} - c^2 \frac{\partial^2 u}{\partial x^2} - \nu^2 \frac{I_p}{F} \frac{\partial^4 u}{\partial x^2 \partial t^2} = 0, \quad (4)$$

where ν denotes Poisson's ratio, I_p is the polar moment of inertia of a rod cross section with area F (for a circle $I_p = \pi d^4/32$), y and z are the distances from the neutral axis to the chosen point of the cross section.

The boundary conditions for this equation are reduced to the same as in the case of the wave equation [11].

To solve equation (4), initial representation (2) can be used. Substituting it into the boundary conditions results in an improved expression for the frequencies of the longitudinal rod vibrations (f_{Rn}) in terms of the corresponding frequencies (f_{wn}) obtained from the solution of the wave equation:

$$f_{Rn} = \frac{f_{wn}}{\sqrt{1 + \eta_n}}, \quad f_{wn} = \frac{nA}{2L}, \quad \eta_n = \frac{\pi^2 n^2 \nu^2 d^2}{8L^2}, \quad n = 1, 2, \dots \quad (5)$$

At a small value of the correction factor in radical expression (5), the correction to the frequency is reduced to the known Rayleigh correction [1].

To compare the values of frequencies calculated by formula (5) with the experimentally measured frequencies, it is necessary to know Poisson's ratio of the rod material in addition to the velocity of longitudinal waves. Reference data on this coefficient for aluminum alloys vary noticeably within 0.31–0.33 [9], 0.32–0.36 [12]. To clarify this value for the material of the tested rod, we use the approach for determining Poisson's ratio suggested in [13].

The essence of the approach is as follows. Setting Poisson's ratio in the possible range of values (0.31–0.36) and calculating the values of the natural frequencies of rod vibrations using formula (5), we obtain a set of calculated frequencies corresponding to the measured experimental frequencies. Then, composing the absolute differences between the experimental and calculated frequencies with the same numbers, summing these differences and dividing by the number of frequencies, we obtain the criterion for the deviation of the calculated values of frequencies from the experimental values at the selected value of Poisson's ratio:

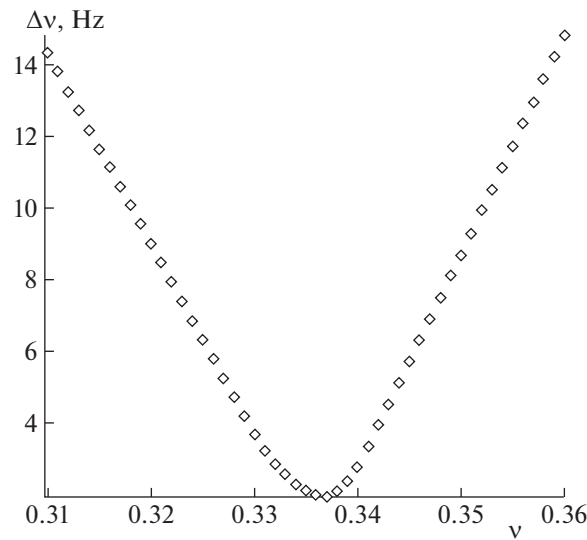


Fig. 3. Determining Poisson’s ratio from the condition of the minimum difference between the sets of experimental and calculated frequencies.

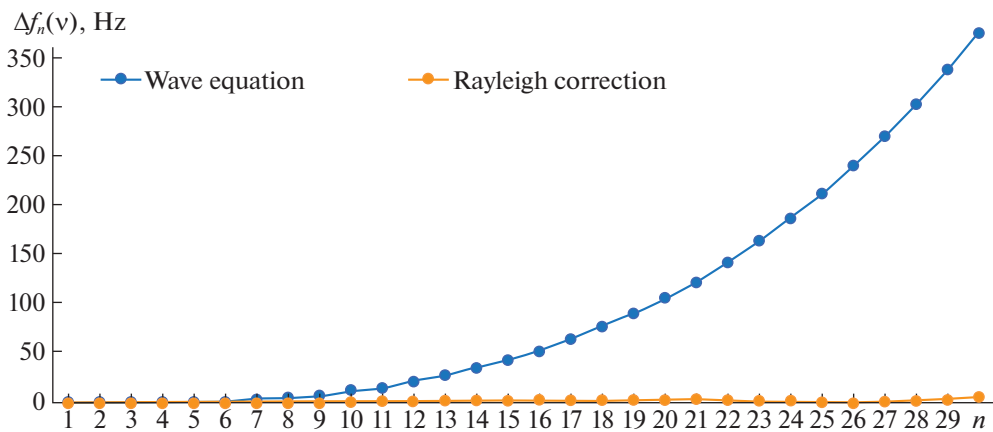


Fig. 4. Differences in Hz between the calculated and experimental frequencies depending on the frequency number.

$$\Delta(\nu) = \frac{1}{N} \sum_{n=1}^N |\Delta f_n(\nu)|, \quad \Delta f_n(\nu) = f_{n,cal}(\nu) - f_{n,exp}(\nu). \tag{6}$$

Figure 3 shows the graph of dependence $\Delta(\nu)$ from which it can be seen that the minimum deviation between the experimental and calculated sets of frequencies occurs at $\nu = 0.337$.

At the chosen value of Poisson’s ratio, we determined 30 natural frequencies of longitudinal vibrations of the rod and their differences from the experimental frequencies. These differences depending on the frequency number are shown in Fig. 4 in comparison with similar differences between the experimental values and the frequencies calculated without the Rayleigh correction.

As can be seen from Fig. 4, the frequencies found by formula (5) almost do not differ from the values of the experimental frequencies in the entire considered range.

It would seem that Eq. (5) almost perfectly describes the longitudinal vibrations of the rod. However, it has a feature that can manifest by eliminating time dependence

$$u(x, t) = X(x) \exp(i\omega t) \tag{7}$$

and grouping the terms of the second derivative of function $X(x)$:

$$\left(1 - v^2 \lambda^2 \frac{I_p}{F}\right) X''(x) + \lambda^2 X(x) = 0. \quad (8)$$

At a certain frequency corresponding to the limiting point of concentration of frequencies (f_{kp}) [14] the coefficient at the highest derivative in Eq. (8) can vanish, and become negative when that frequency is exceeded, which results in non-oscillating solutions of the equation. The estimate of the f_{kp} value for the rod considered in this study gives a value of about 300 kHz, i.e., the maximum frequency (38 557.99 Hz) of the range of the first 30 frequencies of natural vibrations of this rod is almost an order of magnitude lower than the critical frequency, which guarantees the applicability of the Rayleigh correction for calculating even higher frequencies. At the same time, the graph in Fig. 4 shows a certain concentration of the experimental frequencies with an increase in their number and magnitude. Despite this, the fundamental limitation of the frequency spectrum calculated by the Rayleigh correction and the remaining insignificant differences in the values of the experimental and calculated frequencies suggest a transition to the improved model of longitudinal rod vibrations, developed by Bishop.

BISHOP MODEL

The main feature of the Bishop model is considering not only transverse, but also shear deformations [4, 5]. Longitudinal vibrations of the rod according to this model are described by a more complex equation of the 4th order in x :

$$\frac{\partial^2 u}{\partial t^2} - c^2 \frac{\partial^2 u}{\partial x^2} - v^2 \frac{I_p}{F} \frac{\partial^4 u}{\partial x^2 \partial t^2} + \frac{c^2 v^2}{2(1+v)} \frac{I_p}{F} \frac{\partial^4 u}{\partial x^4} = 0. \quad (9)$$

Accordingly, its solution requires two boundary conditions at each end of the rod. Examples of such conditions are presented in [5]. In the case of free ends, they have form

$$\left(EF \frac{\partial u}{\partial x} + v^2 \rho I_p \frac{\partial^3 u}{\partial x \partial t^2} - v^2 G I_p \frac{\partial^3 u}{\partial x^3} \right) \Big|_{x=0,L} = 0, \quad \frac{\partial^2 u}{\partial x^2} \Big|_{x=0,L} = 0, \quad (10)$$

$$G = \frac{E}{2(1+v)}.$$

In the case of rigid fixing of the ends of the rod, the boundary conditions are as follows:

$$u \Big|_{x=0,L} = 0, \quad \frac{\partial u}{\partial x} \Big|_{x=0,L} = 0. \quad (11)$$

The general solution of Eq. (9) is represented by a combination of trigonometric and hyperbolic functions:

$$u(x, t) = (C_1 \cosh \beta_1 x + C_2 \sinh \beta_1 x + C_3 \cos \beta_2 x + C_4 \sin \beta_2 x) \exp(i\omega t), \quad (12)$$

$$\beta_{1,2}^2 = \sqrt{\frac{a^2}{4b^2} + \frac{\lambda^2}{b}} \pm \frac{a}{2b}, \quad a = 1 - v^2 \lambda^2 \frac{I_p}{F}, \quad b = \frac{v^2}{2(1+v)} \frac{I_p}{F}.$$

Substituting (12) into boundary conditions (11) or (10) leads to frequency equations for rigidly fixed ($n = 0$) or free ($n = 1$) ends:

$$2(\beta_1 \beta_2)^{2n+1} \left(\cos \beta_2 L - \frac{1}{\cosh \beta_1 L} \right) + (-1)^n (\beta_2^{4n+2} - \beta_1^{4n+2}) \sin \beta_2 L \tanh \beta_1 L = 0, \quad n = 0, 1. \quad (13)$$

To compare the results for various models of longitudinal rod vibrations, it is convenient to use the boundary conditions for the free stop of the rod ends against rigid walls [15]. In this case, there are no longitudinal displacements and shifts proportional to the second derivative at the edges of the rod:

$$u \Big|_{x=0,L} = 0, \quad \frac{\partial^2 u}{\partial x^2} \Big|_{x=0,L} = 0.$$

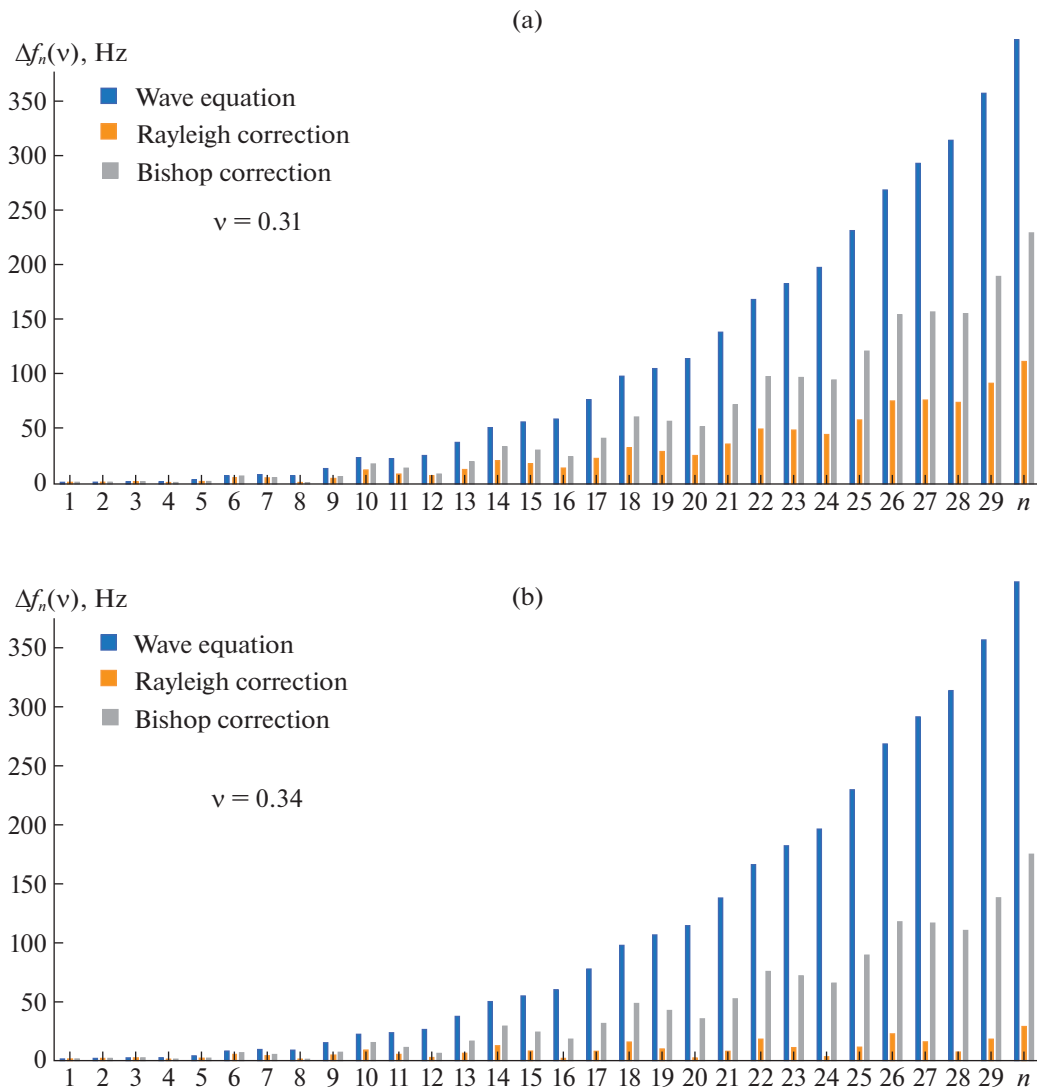


Fig. 5. Differences between the calculated frequencies according to the wave equation and with the Rayleigh and Bishop corrections from the experimental rod frequencies: (a) – at $\nu = 0.31$, (b) – at $\nu = 0.34$.

These conditions make it possible to represent the solution of Eq. (6) in a simple form:

$$u(x, t) = \sin \frac{\pi n x}{L} \exp(i\omega t), \quad n = 1, 2, \dots \tag{14}$$

Therefore, for frequencies f_{Bn} an explicit formula of longitudinal rod vibrations can be written according to the Bishop model:

$$f_{Bn} = f_{Rn} \sqrt{1 + \frac{\eta_n}{2(1 + \nu)}}, \quad n = 1, 2, \dots, \tag{15}$$

where f_{Rn} denotes the frequencies calculated by Rayleigh’s correction (5).

Formula (15) shows that the rod vibration frequencies obtained by the Bishop model should have lower values than those calculated from the wave equation, but exceed the frequencies determined using Rayleigh’s correction. This is clearly confirmed by the diagrams shown in Fig. 5. They show the differences between the calculated frequencies, calculated by the wave equation and with Rayleigh and Bishop corrections using the general boundary conditions of free ends (10) and the experimental frequencies

depending on the frequency number at the smallest possible value of Poisson's ratio and close to the value of $\nu = 0.34$ obtained by algorithm (7).

As can be seen from Fig. 5, while Bishop's correction in the fourth-order equation brings the frequencies of the wave equation closer to the values of the experimental frequencies of longitudinal vibrations of a homogeneous rod, it is to an incomparably lesser extent than the simpler Rayleigh correction, which follows from the equation of the same order as the wave equation. It should also be noted that in the case of a long rod, using the simplest representation (14) to describe the vibration mode of the rod according to the Bishop model leads to the values of the natural vibration frequencies that practically coincide with the frequencies determined from general solution (12) under general boundary conditions (11) (the difference in frequencies is noticeable only in the sixth and seventh significant digits). Consequently, using the more general, but also a much more complex model of longitudinal rod vibrations based on Bishop's corrections not only does not improve, but even worsens the agreement between the calculated and experimental frequencies in the case of a long rod.

CONCLUSIONS

It is widely accepted that the more theoretically possible factors are taken into account in a mathematical model, the more perfect it is and should better agree with experimental data. In this study, using the example of longitudinal vibrations of a rod, three levels of such models were considered: the wave equation, an improved equation that takes into account the effect of the transverse deformation of the rod, and a fourth-order equation in coordinates, taking into account shear deformations in addition to the previous case. The vibration frequency spectra of the rod determined using these models were compared to an experimental set of frequencies obtained using high-precision spectrum analyzing equipment. The result of this comparison turned out to be counter intuitive.

Comparing the experimental frequencies with the frequencies determined by the wave equation model showed their rapidly increasing discrepancy with increasing frequency number. The best agreement with the experimental frequencies was shown by the values calculated with the Rayleigh correction, i.e., the model taking into account the effect of transverse deformation. The frequencies determined by a more complex model developed by Bishop, which takes into account both transverse and shear deformations, somewhat improve the results obtained from the wave equation, but they approximate their values far worse compared to the experiment than frequencies calculated only with transverse deformation. This can be explained by the fundamental property of symmetric deformation of the cross section of the rod during longitudinal vibrations.

It is, of course, possible to consider variants of longitudinal vibrations of rods of a non-symmetric cross section, which would most likely be accompanied by vibrations of other types. In these cases, it is likely that shear deformations would play some role in improving the calculated frequencies of longitudinal vibrations of the rod. However, when calculating the frequencies of longitudinal vibrations for long rods with a symmetric cross section, it is not necessary to transition to a more complex model than the vibration equation with accounting for transverse deformation.

FUNDING

This study was supported by the Russian Foundation for Basic Research (project No. 19-01-00100).

REFERENCES

1. J. V. Strutt (Lord Rayleigh), *The Theory of Sound* (Macmillan and Co., London, 1926; GITTL, Moscow, 1955).
2. A. Love, *Mathematical Theory of Elasticity* (Cambridge Univ. Press, Cambridge, 1927; ONTI, Moscow, 1935).
3. S. P. Timoshenko, *Vibration Problems in Engineering* (Van Nostrand, Toronto, 1955; Nauka, Moskva, 1967).
4. R. E. D. Bishop, "Longitudinal waves in beams," *Aeronautical* **3**, 280–293 (1952).
5. S. S. Rao, *Vibration of Continuous Systems* (Wiley, Hoboken, N.J., 2007).
6. A. Kundt, "Acoustic experiments," *London, Edinburgh, Dublin Philos. Mag. J. Sci.* **35** (4), 41–48 (1868).
7. *Nondestructive Testing and Diagnostics: Handbook*, Ed. by V. V. Klyuev (Mashinostroenie, Moscow, 2003; Metrix Instrument, Houston, Tex., 2004).
8. Functions ZETLAB. <https://zetlab.com/product-category/programmnoe-obespechenie/funksii-zetlab>. Accessed March 4, 2021.

9. A. K. Belyaev, C.-C. Ma, N. F. Morozov, P. E. Tovstik, T. P. Tovstik, and A. O. Shurpatov, “Dynamics of a rod undergoing a longitudinal impact by a body,” *Vestn. St. Petersburg Univ., Math.* **50**, 310–317 (2017).
<https://doi.org/10.3103/S1063454117030050>
10. *Handbook of Physical Quantities*, Ed. by I. S. Grigor’ev and E. Z. Meilikhov (Energoatomizdat, Moscow, 1991; CRC, Boca Raton, Fla., 1997).
11. *Vibration in Technology: Handbook* (Mashinostroenie, Moscow, 1978), **Vol. 1** [in Russian].
12. *Handbook on Strength of Materials*, Ed. by G. S. Pisarenko, A. P. Yakovlev, and V. V. Matveev, (Naukova Dumka, Kiev, 1988) [in Russian].
13. L. D. Akulenko and S. V. Nesterov, *High Precision Methods in Eigenvalue Problems and their Applications* (CRC, London, 2004).
14. I. A. Fedotov, A. D. Polyanin, and M. Yu. Shatalov, “Theory of free and forced vibrations of a rigid rod based on the Rayleigh model,” *Dokl. Phys.* **52**, 607–612 (2007).
15. I. A. Fedotov, A. D. Polyanin, M. Yu. Shatalov, and H. M. Tenkam, “Longitudinal vibrations of a Rayleigh–Bishop rod,” *Dokl. Phys.* **55**, 609–614 (2010).

Translated by L. Trubitsyna

SPELL; OK